# Supporting Information

## Tong *et al.* 10.1073/pnas.0809339106

### SI Methods

**Isolation of DAPK-1 cDNA.** To isolate a full-length DAPK-1 cDNA, we designed primers based on an early predicted gene structure for K12C11.4 and used these in RT-PCR from polyA(+) RNA from mixed-stage animals. The purified products were cloned into pST-Blue vector (Novagen) and confirmed by sequencing. The *dapk-1* ORF is 4275 bp and encodes a 1425 residue polypeptide.

**RNA Interference of Secretion and Endocytosis Genes.** We used postembryonic feeding RNAi to inhibit the following genes: adaptin mu3 (*apm-3*), dynamin (*dyn-1*), Rab1 (*rab-1*), Sec23 (*sec*-23), synaptotagmin (*snt-2*), Vps32 (*vps-32.1*), and Vps54 (*vps-54*), in either *rrf-3(pk1426)* or in *dapk-1(ju469); rrf-3(pk1426)* host strains. Embryos were hatched on plates containing the RNAi bacteria and grown at 25 °C for 3 days before scoring. Because RNAi of some genes (*dyn-1, rab-1, sec*-23, vps-32.1) causes highly penetrant larval lethality, we titrated the RNAi bacteria between 1:10 to 1:100 with control HT115 bacteria to find RNAi levels compatible with viability to the L4 stage.

**Cuticle Fragility Tests.** We tested cuticle strength by measuring time to cuticle rupture in bleach. Day old hermaphrodites were placed in freshly made alkaline hypochlorite solution (1N NaOH, 2% hypochlorite) on a microscope slide and the time to cuticle rupture recorded. Wild type worms typically rupture at the vulva, whereas *dapk-1* mutants ruptured at the regions of cuticle thickening at the head or dorsal midline.

**Microarray Transcriptional Profiling.** RNA was isolated from L4 stage *dapk-1*(*ju4*) animals and hybridized to oligonucleotide arrays essentially as described (1). Data in SI Table S4 show the top 18.75 percentile (of 303 genes) with median fold up-regulation >1.24 across 3 replicates.


1. Pujol N, *et al.* (2008) Anti-fungal innate immunity in *C. elegans* is enhanced by evolutionary diversification of antimicrobial peptides. *PLoS Pathog* 4:e1000105.
2. Tereshko V, Teplova M, Brunzelle J, Watterson DM, Egli M (2001) Crystal structures of the catalytic domain of human protein kinase associated with apoptosis and tumor suppression. *Nat Struct Biol* 8:899–907.
3. Michaux G, Gansmuller A, Hindelang C, Labouesse M (2000) CHE-14, a protein with a sterol-sensing domain, is required for apical sorting in *C. elegans* ectodermal epithelial cells. *Curr Biol* 10:1098–1107.
4. Wong D, Bazopoulou D, Pujol N, Tavernarakis N, Ewbank JJ (2007) Genome-wide investigation reveals pathogen-specific and shared signatures in the response of *Caenorhabditis elegans* to infection. *Genome Biol* 8:R194.

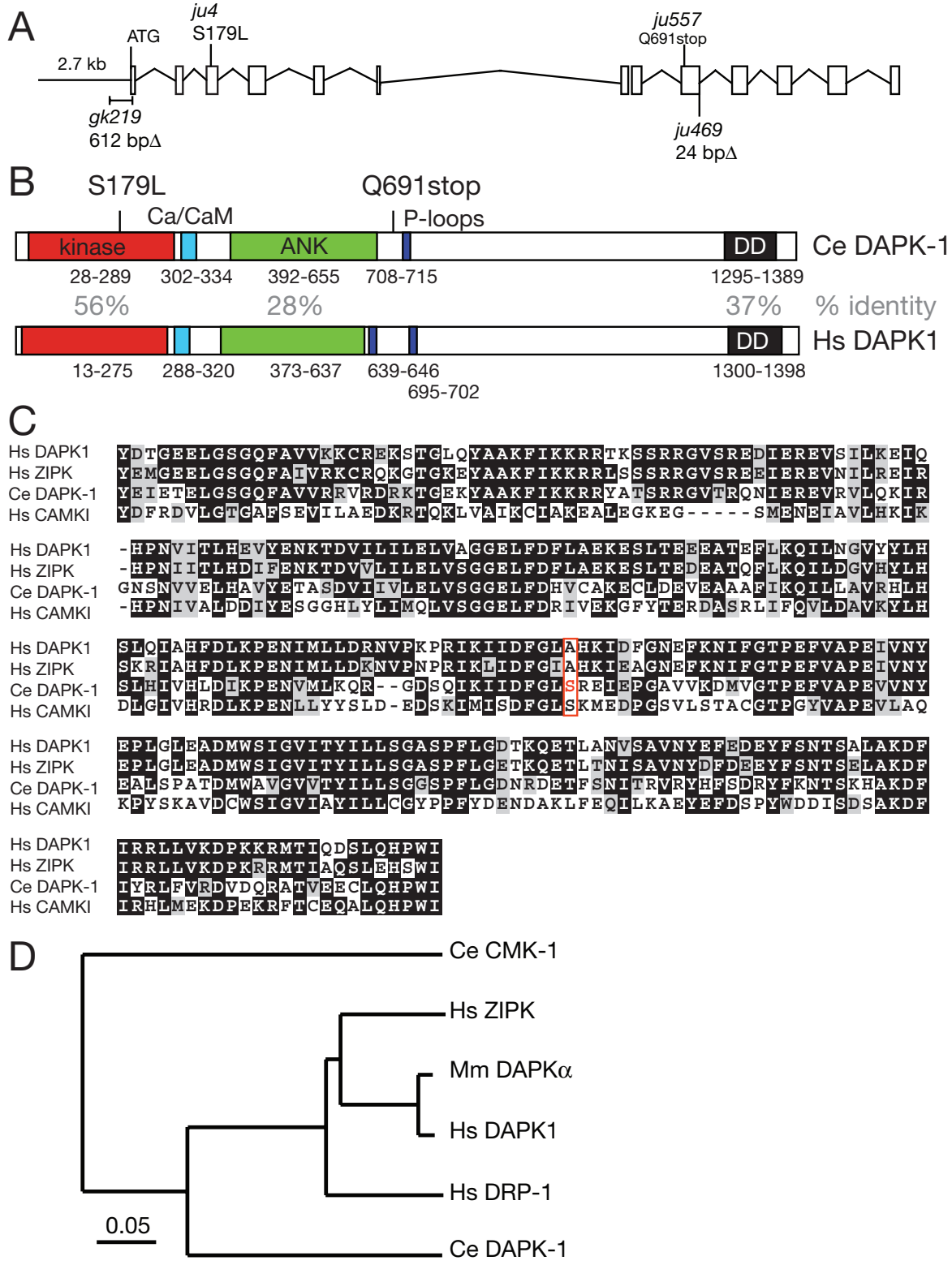


**Fig. S1.** *dapk-1* encodes the *Caenorhabditis elegans* ortholog of death-associated protein kinase (DAPK). (*A*) *C. elegans dapk-1* gene structure showing positions of mutations and the 2.7-kb promoter used in rescuing construct pCZ767; *ju4* results in the missense alteration S179L, and is predicted to affect the substrate binding groove of the kinase domain (2); *gk219* deletes 516 bp of the 5′ UTR and 96 bp of exon 1 (codons 1–32); *ju469* is a 24 bp deletion of the last 10 bp of exon 9 and 14 bp of intron 9; *ju469* is predicted to truncate DAPK-1 after residue 862; *ju557* is a nonsense mutation (Q691stop) in exon 9 after the ANK repeats. (*B*) Comparison of *C. elegans* DAPK-1 to human DAPK1, showing kinase domains (red), $Ca^{2+}$/calmodulin regulatory domain (blue), ANK repeats (green), P-loops (purple), death domain (black), and percentage identity. DAPK-1 is overall 33% identical to human DAPK1. (*C*) Clustal 2.0 alignment of DAPK-1 kinase domain with human DAPK1, human ZIP kinase and human CaM kinase I. S179 (red) corresponds to A165 in human DAPK. (*D*) Phylogenetic tree (ClustalW and njplot) of kinase domains of *C. elegans* DAPK-1, *C. elegans* CaM kinase I/CMK-1, human DAPK1, human ZIP kinase, human DRP-1 and mouse DAPK. DAPK-1 is the only *C. elegans* member of the DAPK family.

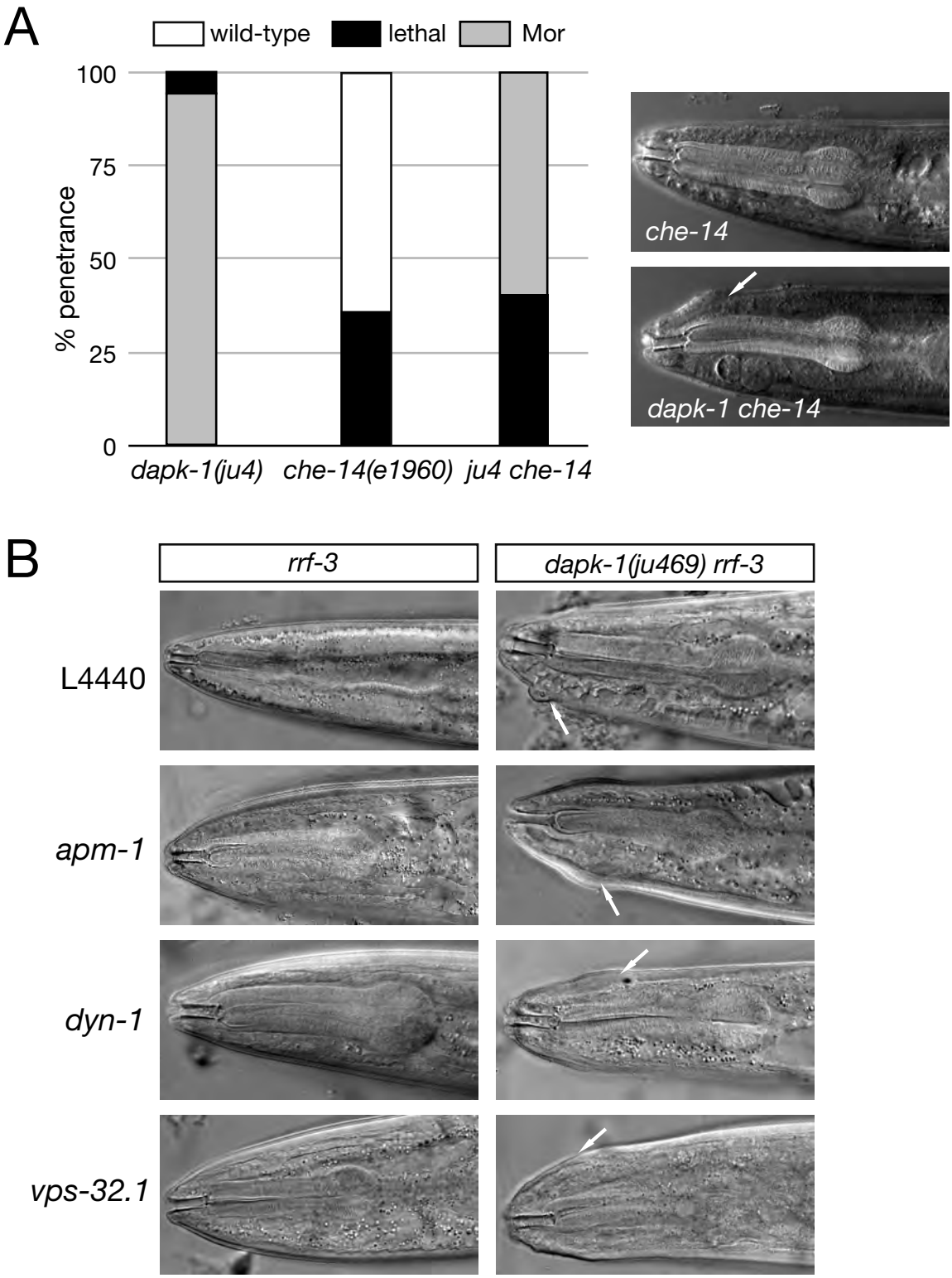


**Fig. S2.** The *dapk-1* phenotypes are not phenocopied, enhanced, or suppressed by loss of function in epithelial endocytosis or secretion pathways. (*A*) The *dapk-1*(*ju4*) *che-14*(*e1960*) double mutants display additive epidermal and lethal phenotypes; *che-14* encodes a Ptc family protein involved in apical secretion by the epidermis (3) ($n > 500$, animals for each genotype). Arrow indicates the head morphology (Mor) defect of *dapk-1* mutants. (*B*) Photomicrographs of head morphology in RNAi experiments inhibiting genes in the secretory or endocytic pathways. The effects of postembryonic feeding RNAi of the indicated gene are shown in *rrf-3* and in *dapk-1*(*ju469*) *rrf-3* backgrounds. We observed no detectable suppression or enhancement of the *dapk-1* phenotypes.

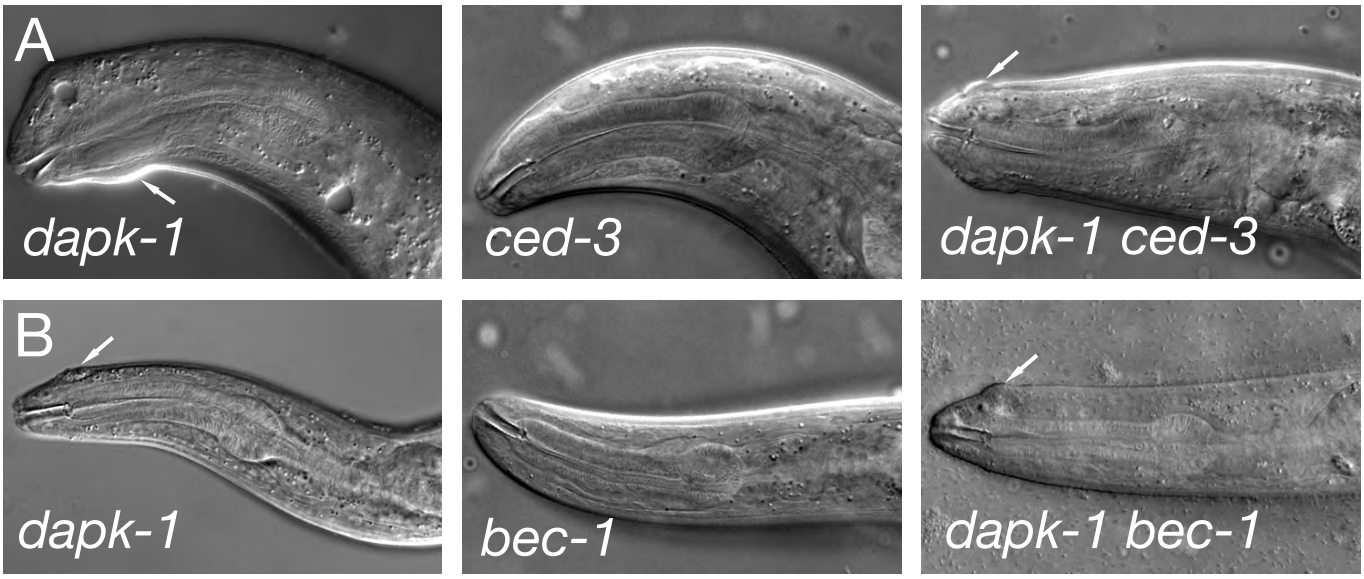


**Fig. S3.** Lack of genetic interaction of *dapk-1* with apoptosis or autophagy mutants in head morphogenesis. (*A*) Nomarski DIC micrographs of head morphology of adult *dapk-1*(*ju4*), *ced-3*(*n717*), and *ju4; n717* double mutants, showing *ced-3* neither phenocopies nor suppresses *dapk-1* epidermal morphology defects (arrows). (*B*) The *bec-1* mutants neither phenocopy nor suppress the *dapk-1* epidermal defects (arrows). As most *ok700* animals arrest in larval development, images are of L4 stage head region of *bec-1*(*ok700*) and *dapk-1; bec-1* double mutants. See Table S2 for quantitation.

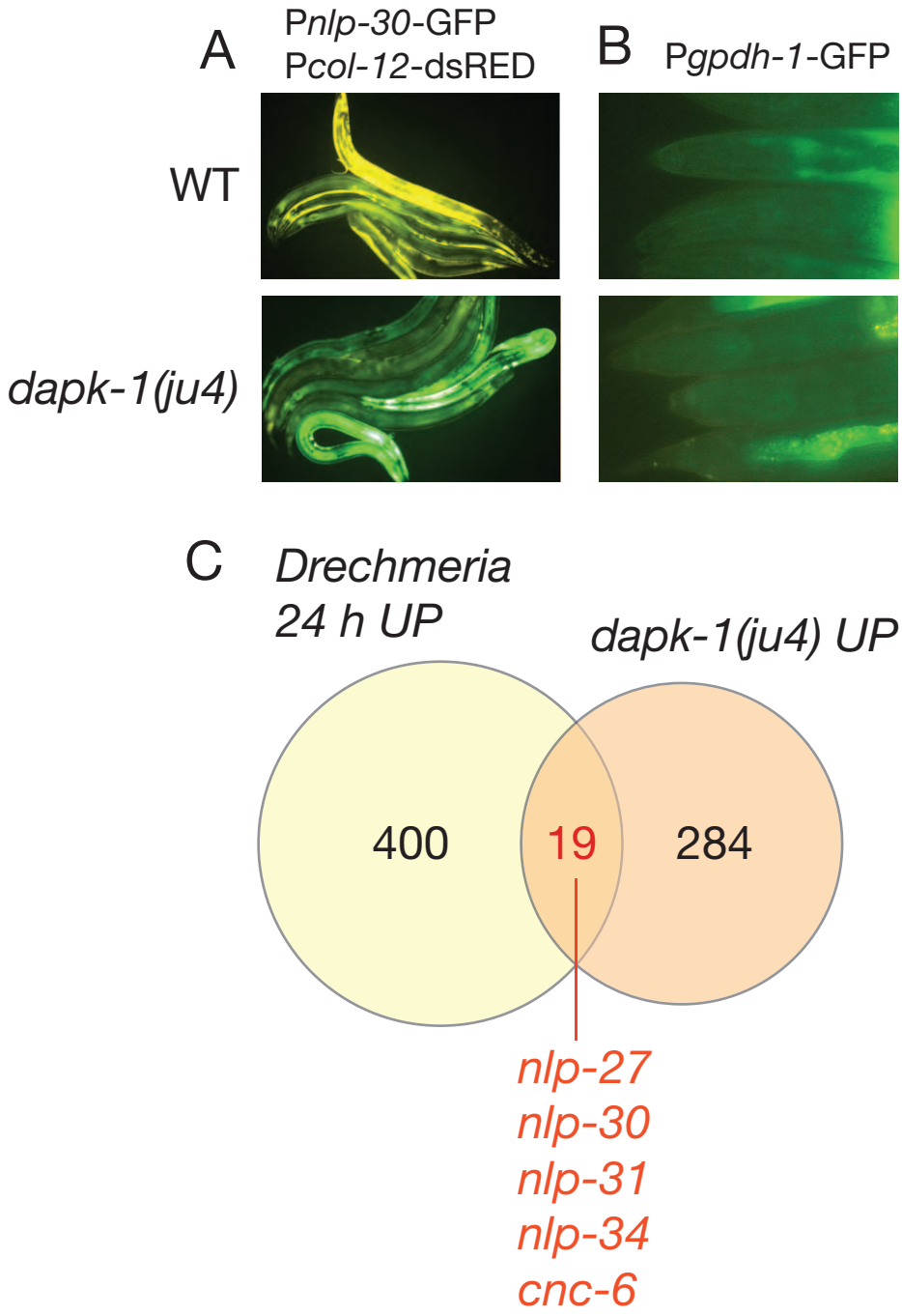


**Fig. S4.** Up-regulation of cutaneous innate immune response but not osmotic stress response in *dapk-1* animals. (*A* and *B*) Expression of P*nlp-30*-GFP/P*col-12*-dsRed (*A*) in day 1 adults and (*B*) P*gpdh-1*-GFP *kbIs5* in L4 stage wild type and *dapk-1*(*ju4*). Animals were photographed under identical camera settings. Residual fluorescence in the P*gpdh-1*-GFP panels is due to gut autofluorescence. (*C*) Venn diagram of overlap between top-quartile *dapk-1*(*ju4*) up-regulated genes (303 genes) and *Drechmeria* infected worms (24 h, 419 genes). The 19 genes in common, listed in Table S4, include the AMPs *nlp-27*, *nlp-30*, *nlp-31*, *nlp-34*, and *cnc-6*. None of the 303 genes up-regulated in *dapk-1* are in the 254 genes of the bacterial ''common response'' (4).

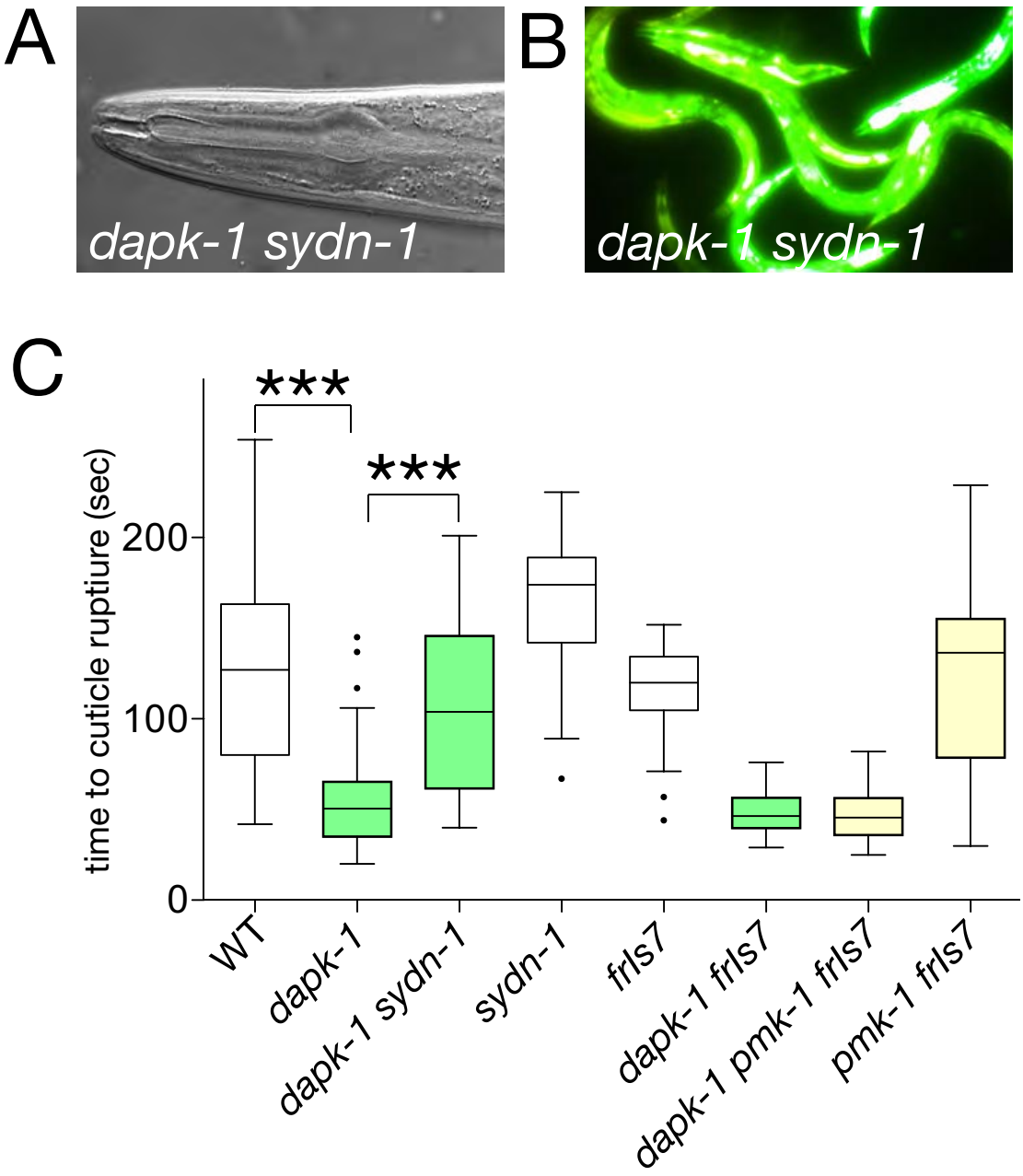


**Fig. S5.** Genetic suppression of *dapk-1* indicates up-regulation of AMPs is independent of morphological defects. (*A* and *B*) The *dapk-1*(*ju4) sydn-1*(*ju541*) double mutants have normal head morphology (*A*) and up-regulated P*nlp-29*-GFP (*B*). (*C*) The *dapk-1* cuticle fragility defects are suppressed by *sydn-1* but not by *pmk-1*; Tukey boxplots ($n = 50$, for each genotype); tests of significance use *t* test, $P < 0.001$.

**Table S1. Quantitation of *dapk-1* morphogenetic phenotypes**

| Genotype, temperature | Morphological defect, % | *n* |
|---|---|---|
| *dapk-1*(*ju4*) 25 °C | 100 | 538 |
| *dapk-1*(*ju4*) 20 °C | 100 | 309 |
| *dapk-1*(*ju4*) 15 °C | 98 | 454 |
| *dapk-1*(*ju469*) 25 °C | 42 | 632 |
| *dapk-1*(*ju469*) 20 °C | 16 | 280 |
| *dapk-1*(*ju469*) 15 °C | 12 | 253 |
| *dapk-1*(*ju557*) 25 °C | 79 | 507 |
| *dapk-1*(*ju557*) 20 °C | 33 | 183 |
| *dapk-1*(*ju557*) 15 °C | 23 | 262 |
| *dapk-1*(*gk219*) 25 °C | 65 | 743 |
| *dapk-1*(*gk219*) 20 °C | 19 | 281 |
| *dapk-1*(*gk219*) 15 °C | 12 | 222 |

The *dapk-1* alleles form an allelic series, in order of phenotypic severity: *ju4* > *ju557* > *gk219* > *ju469*. All 4 alleles are temperature-sensitive, suggesting loss of *dapk-1* function reveals an underlying temperature-sensitive process.

**Table S2. *dapk-1* double mutants**

| Genotype | Morphological defect, % | *n* |
|---|---|---|
| *dapk-1*(*ju4*) | 100 | 538 |
| *dapk-1*(*ju4*) *unc-54*(*e190*)* | 100 | 112 |
| *dapk-1*(*ju4*); *ced-3*(*n717*) | 100 | 606 |
| *dapk-1*(*ju4*); *ced-2*(*e1752*) | 100 | 538 |
| *dapk-1*(*ju469*) | 42 | 632 |
| *dapk-1*(*ju469*); *ced-3*(*n717*) | 89 | 294 |
| *dapk-1*(*ju469*); *ced-2*(*e1752*) | 90 | 476 |
| *dapk-1*(*ju4*); *bec-1*(*ok700*)* | 100 | 53 |
| *dapk-1*(*ju4*); *atgr-18*(*gk378*)* | 100 | 231 |
| *dapk-1*(*gk219*); *unc-51*(*e369*) | 93 | 268 |
| *dapk-1*(*ju4*); *pmk-1*(*km25*)* | 100 | 666 |
| *dapk-1*(*ju4*); *sek-1*(*km4*)* | 100 | 271 |
| *dapk-1*(*ju4*); *nsy-1*(*ky397*) | 98 | 333 |
| *dapk-1*(*ju4*); *tir-1*(*tm3036*), 20 °C | 100 | 656 |
| *dapk-1*(*ju4*); *sydn-1*(*ju541*) | 0 | 513 |

Double mutants were scored at 25 °C or at room temperature (22–23 °C) (indicated by asterisks). Non-*dapk-1* single mutants have normal epidermal morphology. Because *dapk-1* partial loss of function mutants (*ju469, gk219*) are mildly enhanced by mutations that either prevent apoptosis, autophagy, or phagocytosis, these enhancement effects may reflect a nonspecific effect of overall sickness, or may reflect a cryptic role for all three processes in epidermal morphogenesis.

**Table S3. Transgenic rescue of *dapk-1***

| Genotype | Morphological defect, % | *n* |
|---|---|---|
| *dapk-1*(*ju4*) | 100 | 538 |
| *dapk-1*(*ju4*); *juEx886* [*Pdapk-1-DAPK-1*] | 10 | 62 |
| *dapk-1*(*gk219*) | 65 | 743 |
| *dapk-1*(*gk219*); *juEx890* [*Pdapk-1-DAPK-1*] | 2 | 125 |
| *dapk-1*(*gk219*); *juEx891* [*Pdapk-1-DAPK-1*] | 1 | 207 |
| *dapk-1*(*ju4*); *juEx1681* [*Pdpy-7-DAPK-1*] | 19 | 317 |
| *dapk-1*(*ju4*); *juEx1682* [*Pdpy-7-DAPK-1*] | 3 | 260 |
| *dapk-1*(*ju4*); *juEx921* [*Pdapk-1-GFP*::*DAPK-1*] | 8 | 107 |
| *dapk-1*(*gk219*); *juEx924*[*Pdapk-1-GFP*::*DAPK-1*] | 0 | 160 |

All transgenic lines were scored at 25 °C. The transgenic rescue of *ju4* or *gk219* by all full-length DAPK-1 transgenes is highly significant by the Fisher exact test (data not shown).

**Table S4. Genes upregulated in *dapk-1* and in *Drechmeria* infected worms**

| Gene | Median fold *dapk-1* | Median fold infected | Function |
|---|---|---|---|
| B0213.17 *nlp-34* | 2.55 | 3.34 | AMP |
| B0213.2 *nlp-27* | 1.34 | 1.53 | AMP |
| B0213.5 *nlp-30* | 1.68 | 2.78 | AMP |
| B0213.6 *nlp-31* | 1.28 | 2.51 | AMP |
| C06A8.3 | 1.39 | 1.18 | — |
| C06G4.2a *clp-1* | 1.48 | 1.20 | Calpain |
| C13A10.2 | 1.26 | 1.23 | — |
| C45B2.8 | 1.39 | 1.65 | — |
| F19B6.1b | 1.34 | 1.25 | plakoglobin-like |
| F36H12.5 | 1.33 | 1.26 | — |
| F55H12.4 | 1.36 | 2.25 | — |
| K02F6.6 | 1.25 | 1.20 | BTB/POZ domain |
| R13A5.6 *ttr-8* | 1.28 | 1.24 | Transthyretin |
| T19B10.2 *phi-59* | 1.24 | 1.84 | — |
| Y46E12A.1 *cnc-6* | 1.73 | 1.85 | AMP |
| Y53G8AR.6 | 1.35 | 1.25 | SAP domain |
| Y54G11A.9 | 1.49 | 1.25 | — |
| Y71H2AM.18 | 1.29 | 1.18 | DEAD box |
| ZK637.14 | 1.44 | 1.33 | RING finger |

Common genes from the top quartiles of up-regulated genes. Data from *Drechmeria* infected worms are 24 h post infection (1).